

Magnetic and Dielectric Properties in Multiferroic $\text{Cu}_3\text{Mo}_2\text{O}_9$ under High Magnetic Fields

Haruhiko KUROE¹, Kento AOKI¹, Ryo KINO¹, Tasuku SATO¹, Hideki KUWAHARA¹, Tomoyuki SEKINE¹, Takumi KIHARA², Mitsuru AKAKI², Yoshimitsu KOHAMA², Masashi TOKUNAGA², Akira MATSUO², Koichi KINDO², Masashi HASE³, Kanji TAKEHANA³, Hideaki KITAZAWA³, Kunihiko OKA⁴, Toshimitsu ITO⁴, and Hiroshi EISAKI⁴

¹ *Physics Division, Sophia University, 7-1 Kioi-cho, Chiyoda-ku, Tokyo 102-8554, Japan*

² *The Institute for Solid-State Physics (ISSP), the University of Tokyo, Kashiwa, Chiba 277-8581 Japan*

³ *National Institute for Materials Science (NIMS), Tsukuba, Ibaraki 305-0047, Japan*

⁴ *National Institute of Advanced Industrial Science and Technology (AIST), Tsukuba, Ibaraki 305-8568, Japan*

E-mail: kuroe@sophia.ac.jp

(Received September 30, 2013)

The magnetic and dielectric properties under high magnetic fields are studied in the single crystal of $\text{Cu}_3\text{Mo}_2\text{O}_9$. This multiferroic compound has distorted tetrahedral spin chains. The effects of the quasi-one dimensionality and the geometrical spin frustration are expected to appear simultaneously. We measure the magnetoelectric current and the differential magnetization under the pulsed magnetic field up to 74 T. We also measure the electric polarization versus the electric field curve/loop under the static field up to 23 T. Dielectric properties change at the magnetic fields where the magnetization jumps are observed in the magnetization curve. Moreover, the magnetization plateaus are found at high magnetic fields.

KEYWORDS: magnetization plateau, multiferroic material, geometrical spin frustration

1. Introduction

The multiferroic behavior, especially the spin-driven ferroelectricity, is one of the most recent topics in solid-state physics. In a multiferroic phase, where a long-range magnetic order coexists with a ferroelectricity, both of the time reversal and the spatial inversion symmetries are broken. In many spin-driven multiferroic materials, including the first reported material of this class TbMnO_3 [1], the origin of the electric polarization is explained by the spin-current model [2–4]. In this model, a magnetic superlattice formation plays an essential role in breaking these symmetries. Also, the geometrical spin frustration effect, itself, gives a potential to cause a multiferroic behaviour. The ground state of a perfectly frustrated system is characterized as a macroscopically degenerated one. When this degeneracy is lifted, the low-energy excited states appear. These low-energy states lead to field-induced successive phase transitions. The simplest example of this class is an antiferromagnetic (AFM) spin triangle, where a electric polarization is predicted to appear [5, 6].

We have studied the multiferroic properties in $\text{Cu}_3\text{Mo}_2\text{O}_9$ [7]. This compound has the spin frustrating quasi-one dimensional distorted tetrahedral quantum spin system made from $S = 1/2$ Cu^{2+} spins at three different Cu sites, namely Cu1-Cu3. The successive studies of this system were proceeded under the recognition that the canted AFM phase is formed below $T_N = 8.0$ K [8, 9]. The high-quality large single crystals prepared with the continuous solid-state crystallization method enabled us to measure various physical quantities with variety of measuring techniques [10]. The results

of the neutron scattering under zero magnetic field show that there is no sign of the magnetic superlattice formation below T_N and the spin excitations have two interacting branches of the quasi-one-dimensional spinon excitations mainly from the spins at the Cu1 sites with the dominant excitation energy of 4.0 meV in the chain direction and of the nondispersive excitations of the Cu2-Cu3 spin (nearly singlet) dimers at 5.8 meV [11, 12].

The whole dispersion curves of the magnetic excitations at 0 T were reproduced by the bond-operator theory based on the picture of the classical spin wave of the spins at the Cu1 sites interacting with the Cu2-Cu3 quantum spin dimers [13]. This theory predicted a jump of magnetization M accompanied by a drastic change of the ferroelectric polarization P in the narrow region of the magnetic field H ($|H| \sim 50$ T) where the quantum spin dimers are magnetized. Motivated by this prediction, we measured M and P of the single crystals of $\text{Cu}_3\text{Mo}_2\text{O}_9$ under high magnetic fields.

2. Experiments and Results

2.1 Magnetization and electric polarization under pulsed magnetic fields

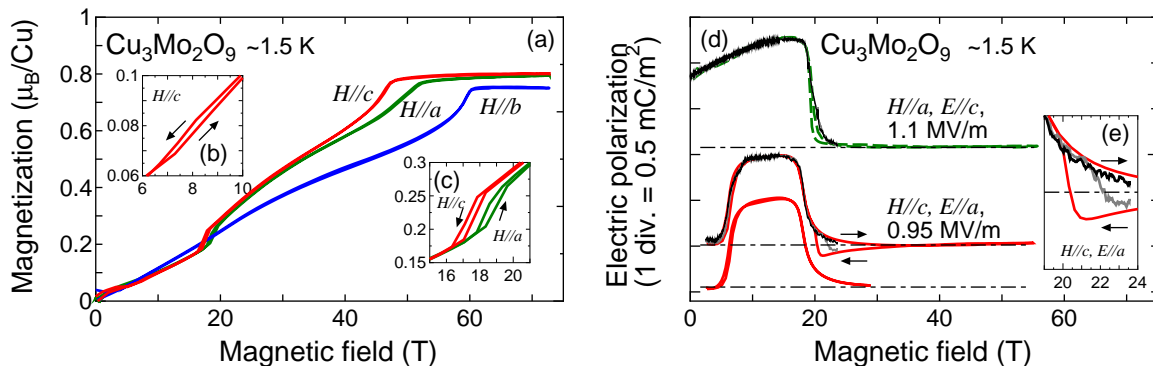


Fig. 1. (color online) The magnetization curves up to 74 T (a) and their expansions (b) and (c). The colors distinguish the directions of magnetizations. The electric polarizations along the a (c) axis as functions of the magnetic field along the c (a) axis are shown by red solid (green dashed) curves in (d) and (e). The dot-dashed lines in (d) and (e) denote the zero electric polarization. The black and gray curves in (d) and (e) show the magnetic field dependence of the electric polarization at a given electric field obtained from the electric polarization-electric field loop. The arrows distinguish the field-increasing and the field-decreasing processes.

The magnetization curves $M(H)$ at 1.5 K in Fig. 1(a) were obtained from their derivatives by using the nondestructive pulsed magnets up to 74 T in the International MegaGauss Science Laboratory, Institute for Solid State Physics (ISSP), the University of Tokyo. The absolute values are obtained by comparison of the data with the ones taken under static magnetic fields [7, 14]. Hereafter, we introduce the subscript x ($x = a, b,$ and c) for the x -component of a vector quantity. As shown in Figs. 1(b) and 1(c), the phase boundaries together with the jumps of M_c (M_a) at 8 and 17 T (19 T) [7, 14, 15] were reproduced well.

Unexpectedly, we observed clear magnetization plateaus at high magnetic fields. The lower boundary of the magnetization plateaus in M_a , M_b , and M_c are 52.3, 60.3, and 47.5 T, respectively. And the values of M_a , M_b , and M_c at these magnetic fields are 0.775, 0.757, and 0.786 in the unit of Bohr magneton μ_B , respectively. These plateaus correspond to the $2/3$ one, when we suppose the anisotropic g values (g_a, g_b, g_c) as (2.33, 2.27, 2.36). We consider that these g values are reasonable because the g value of a polycrystalline sample at low temperature ($g = 2.52$ below 8 T and 2.41 above 8 T, ref. [15]) is larger than the one at room temperature [$(g_a, g_b, g_c) = (2.090, 2.193, 2.180)$]

for single crystal [8] and $g = 2.11$ for polycrystalline sample [15]]. The deviation of the absolute values is probably explained by the drastic changes of the low-temperature ESR spectrum; especially, the reduction of g value above 18 T is caused by the magnetic-field-induced phase transition. Further study of the magnetization curves and ESR spectra up to the saturation magnetic fields are necessary to confirm that these magnetic plateaus correspond to the $2/3$ one.

The P_c - H_a and P_a - H_c curves in Fig. 1(d) were obtained by the integration of the magnetoelectric current under a static electric field and the pulsed magnetic field up to 55 T using another pulsed magnet in ISSP. The P_c - H_a curve was measured under the static electric field of 1.1 MV/m. At 0 T, P_c has a finite value. This reflects the spontaneous electric polarization along the c axis [16]. The P_c increases with increasing magnetic field, saturates around 15 T, and shows a rapid drop around 20 T. The magnetic-field hysteresis effects appear in both of P_c and M_a , as shown in Figs. 1(c) and 1(d). And then, we consider that the changes of P_c and M_a occur simultaneously.

The P_a - H_c curve was measured under the static electric field of 0.95 MV/m, slightly weaker than the case of the P_c - H_a curve. The rapid increase of P_a around 7 T has been reported before [7]. The P_a shows a rapid drop at 18 T. These changes correspond to the magnetic-field-induced phase transitions accompanied by a jump of M_c . The P_a - H_c curve shows a unique magnetic field dependence: We observed that the sign of P_a is flipped only in the field-decreasing process after the maximum magnetic field larger than the lower boundary of the magnetization plateau. The sign flipping of P_c was not observed in the P_c - H_a curve.

2.2 Electric polarization versus electric field loop under static magnetic fields

To discuss the flipping of P_c , the detailed analysis of the P - E loop is necessary. And then, we measured it under the static magnetic field up to 23 T by using the hybrid magnet installed at the National Institute for Material Science. The P - E loops under static H were obtained by using the modified Sawyer-Tower circuit with a measurement frequency of 1 Hz. We numerically subtracted the noise from the power line coming through the ground loop and the signal above T_N which contained the capacitance coming from the sample shape and the coaxial cables.

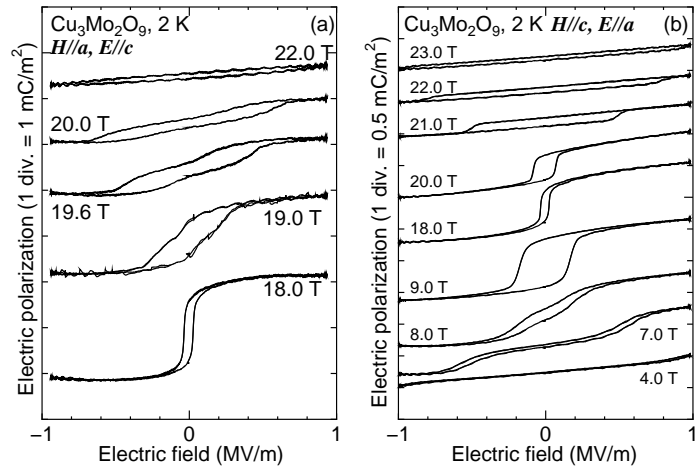


Fig. 2. The electric polarization P_c (P_a) along the c (a) axis versus electric field loops in $\text{Cu}_3\text{Mo}_2\text{O}_9$ under static magnetic field H_a (H_c) along the a (c) axis. Parentheses denote the case of Fig. 2(b).

The typical data around the phase boundaries are shown in Figs. 2(a) and 2(b). At $H_a \sim 18$ T, where the jump of M_a is observed, the P_c - E_c loop shows a drastic change: The double-hysteresis loop is observed at 19.6 and 20.0 T. The small loop observed at 22.0 T is probably a part of the double hysteresis loop. Because the saturated electric field at 22.0 T is larger than the maximum value in this experiment, the double hysteresis loop could be observed as a weak and widely spread P_c - E_c loop.

As shown in Fig. 2(b), the P_a - E_a loop at 4 T is (almost) closed. The double hysteresis loop is observed at 7 T as a precursor of the ferroelectric transition around $H_c \sim 8$ T [7]. The change of the P_a - E_a loop around 18 T is different from the one at 8 T; the coercive electric field (CEF) starts to diverge and the spontaneous electric polarization is suppressed. These changes and the jump of M_c characterize the magnetic-field-induced phase transition at 19 T. At 23 T, the P_a - E_a loop seems to be closed because the CEF is larger than the maximum electric field of the measurements.

To compare with the P - H curve obtained from the magnetoelectric current, we drew the corresponding curve from the P_c - E_c (P_a - E_a) loops under many static H_a (H_c) as the series of P_c (P_a) at a given E_c (E_a). The typical data are shown by black and gray curves in Figs. 1(d) and 1(e). This method has the advantage of detecting the metastable state. We can distinguish the electric polarization in the electric-field increasing and decreasing processes. As shown in Fig. 1(d), the P_a - H_c curve obtained from this procedure reproduces the one from the magnetoelectric current well. However, as shown in Fig. 2(e), we observed a small discrepancy between them around 22 T. It is probably due to the scan speed of H_c and slight difference of E_a .

3. Discussion

3.1 Phase boundaries around 20 T

We emphasize that the way how the P - E loop changes is important. In the standard Landau theory of the temperature-induced first-order phase transition, as is well known, the free energy is expanded up to the sixth-order term of order parameter. The coefficient of the squared order parameter plays an essential role: The phase transition is driven by a change in sign of this. Merz introduced the dimensionless (electric) polarization, the dimensionless electric field, and the dimensionless temperature to obtain the universal curve/loop of the first-order ferroelectric phase transition [17]. According to this theory, there is a parameter region where the double hysteresis loop exists.

In many cases, the coefficient of the squared order parameter is treated to depend only on temperature. However, this can depend on another physical quantity; for example, this coefficient depends on pressure when the phase transition is driven by the change of lattice constant induced by a thermal expansion. In this case, the coefficient of the squared order parameter depends on pressure. In some conditions the pressure-induced phase transition is possible. In case of the magnetization of $\text{Cu}_3\text{Mo}_2\text{O}_9$, the hydrostatic pressure causes the change of effective temperature [9]. In the present work, at $H_c \sim 8$ T and at $H_a \sim 20$ T, we observed the magnetic-field induced phase transitions together with the double hysteresis loop. The origin of these phase transitions is thought to be a change in sign of the squared order parameter under the magnetic field. One of the possible origins is the introduction of the term of $M_x^2 P_{x'}^2$, which is the lowest-order cross-correlation term having an even parity for both of the spatial inversion and the time-reversal symmetry operations.

We did not observe the double hysteresis loop but the diverge of CEF through the phase transition at $H_c \sim 18$ T. Moreover, two P_a - H_c curves obtained from the magnetoelectric current and the P_a - E_a loops under static magnetic fields show similar magnetic-field dependences to each other. And then, we consider that the observation of the flipping of P_a under H_c is related to the observation of P - E loop. As shown in Figs. 2(a) and 2(b), the diverge of CEF was not observed at other phase transitions. Because neither the flipping of electric polarization nor the diverge of CEF are observed in conventional dielectric materials, we conclude that the phase around 20 T is not a conventional paraelectric one. Hereafter, we name this phase the strong CEF phase. The phase transition to the strong CEF phase was reported in the 5.0% Zn-substituted $\text{Cu}_3\text{Mo}_2\text{O}_9$ [18]. In this case, the strong CEF phase appears at 0 T. We consider that the origin of these two CEF phases is important to understand the multiferroic phase in $\text{Cu}_3\text{Mo}_2\text{O}_9$.

3.2 Magnetization curve with magnetization plateau

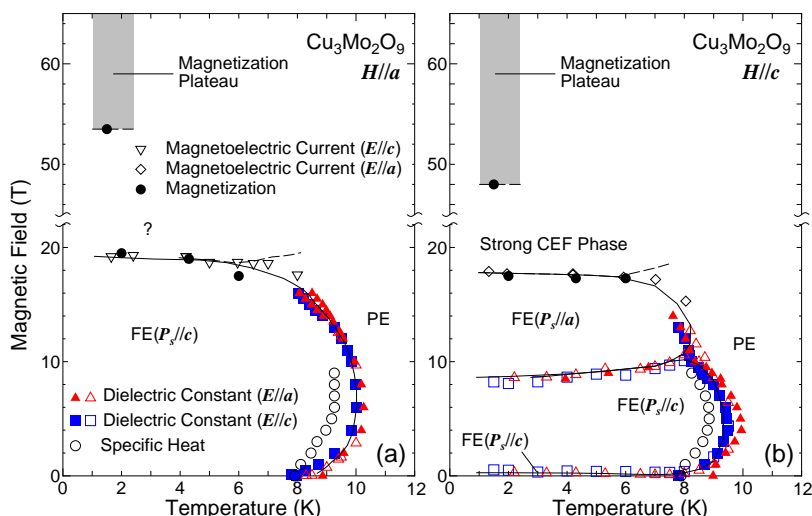
To realize the magnetization more than $1/3$ of the full moment, the Cu2-Cu3 spin dimers should be magnetized, at least partially. It is important to clarify the way how the spin dimers are magnetized in order to understand the magnetization plateau. The present results of magnetization indicate that the Cu2-Cu3 spin dimers start to be magnetized under weaker magnetic field than the theoretically expected value [13]. We need to introduce an additional term into the magnetic Hamiltonian to stabilize the magnetization plateau. It may be explained by the theory in the three-dimensional geometrically frustrated AFM pyrochlore lattice. The biquadratic term added into the standard bilinear Heisenberg AFM Hamiltonian induced by spin-lattice coupling leads to the magnetization plateau [19, 20].

The lower boundaries of the magnetization plateaus in M_a , M_b , and M_c should be the phase boundaries of the quantum phase transition induced by the external magnetic field because the magnetic excitation gap should open in the regions of magnetization plateau. As the examples of magnetic structures with the $2/3$ magnetization, based on the picture of valence bond solid, one can imagine the following: (i) All of the spins at the Cu1 spin-chain sites and a half of the Cu2-Cu3 spin dimers are fully magnetized ($S = 1$) and the rest of the Cu2-Cu3 spin dimers stays singlet ($S = 0$), i.e., the Wigner crystal of $S = 1$ magnetically excited states (the triplon state) is formed; (ii) All of Cu2-Cu3 spin dimers are fully magnetized ($S = 1$) and all of the spins at the Cu1 sites are dimerized to become nonmagnetic ($S = 0$). In the model (ii), the lattice distortion coming from the strong spin-lattice coupling is necessary. This effect is known as the spin-Peierls transition [21], which is observed in the inorganic quantum spin system [22]. The study on the detailed magnetic structures under the magnetization plateau region is strongly desired.

3.3 Phase diagram

We show the H_c - T and H_a - T phase diagrams with the phase boundaries obtained from the present experiments, of which detailed results are not shown here, and our previous ones in refs. [7, 16] in Figs. 3(a) and 3(b), respectively. One can see from Fig. 3(a) that the phase boundaries just below 20 T obtained from the magnetic-field dependences of the magnetization and the electric polarization in this work and ref. [9] connect to the ones around 8 K obtained from the temperature dependence of the specific heat [14] and the dielectric constant [7, 16]. And consequently, we settle the regions of multiferroic phases.

Fig. 3. (color online) The phase diagrams of the magnetic field along the a axis (a) and the c axis (b). Symbols distinguish the experimental methods to obtain the phase boundary. The solid and the dashed curves are only guides for the eye.



The P_a - H_c curve indicates that the phase above 20 T is not the paraelectric phase but the strong CEF phase. The phase boundary between this phase and the paraelectric phase at high temperatures has not been observed yet. At present, as well as in the H_c - T phase diagram, we expect that there is a similar phase boundary in the H_a - T one. It should be confirmed experimentally. Very recent thermodynamical measurements under the pulsed magnetic field clarified this phase boundary [23].

The present work is an interim report of the multiferroic properties of $\text{Cu}_3\text{Mo}_2\text{O}_9$ under high magnetic fields. The detailed phase boundaries above 20 T, including the lower boundary of the magnetization plateau at different temperatures, and the magnetization curves up to the saturated magnetic field are interesting topics which should be clarified in future.

Acknowledgement

We acknowledge Prof. S. Mitsuda in Tokyo University of Science for his technical supports and Dr. N. Terada in NIMS for helpful discussion. This work was supported by Grants-in-Aids for Scientific Research (B, No. 23340096) and (C, No. 22540350) of The Ministry of Education, Culture, Sports, Science, and Technology, Japan.

References

- [1] T. Kimura, T. Goto, H. Shintani, K. Ishizawa, T. Arima, and Y. Tokura: *Nature* **426** (2003) 55.
- [2] H. Katsura, N. Nagaosa, and A. V. Balatsky: *Phys. Rev. Lett.* **95** (2005) 057205.
- [3] M. Kenzelmann, A. B. Harris, S. Jonas, C. Broholm, J. Schefer, S. B. Kim, C. L. Zhang, S.-W. Cheong, O. P. Vajk, and J. W. Lynn: *Phys. Rev. Lett.* **95** (2005) 087206.
- [4] M. Mostovoy: *Phys. Rev. Lett.* **96** (2006) 067601.
- [5] L. N. Bulaevskii, C. D. Batista, M. V. Mostovoy, and D. I. Khomskii: *Phys. Rev. B* **78** (2008) 024402.
- [6] D. I. Khomskii: *J. Phys.: Condens. Matter* **22** (2010) 164209.
- [7] H. Kuroe, T. Hosaka, S. Hachiuma, T. Sekine, M. Hase, K. Oka, T. Ito, H. Eisaki, M. Fujisawa, S. Okubo, and H. Ohta, *J. Phys. Soc. Jpn.* **80** (2011) 083705.
- [8] T. Hamasaki, N. Ide, H. Kuroe, T. Sekine, M. Hase, I. Tsukada, and T. Sakakibara: *Phys. Rev. B* **77** (2008) 134419.
- [9] T. Hamasaki, H. Kuroe, T. Sekine, M. Akaki, H. Kuwahara, and M. Hase: *J. Phys.: Conf. Ser.* **200** (2010) 022013.
- [10] K. Oka, T. Ito, H. Eisaki, M. Hase, T. Hamasaki, H. Kuroe, and T. Sekine, *J. Cryst. Growth.* **334** (2011) 108.
- [11] H. Kuroe, T. Hamasaki, T. Sekine, M. Hase, K. Oka, T. Ito, H. Eisaki, and M. Matsuda: *J. Phys.: Conf. Ser.* **200** (2010) 022028.
- [12] H. Kuroe, T. Hamasaki, T. Sekine, M. Hase, K. Oka, T. Ito, H. Eisaki, K. Kaneko, N. Metoki, M. Matsuda, and K. Kakurai: *Phys. Rev. B* **83** (2011) 184423.
- [13] M. Matsumoto, H. Kuroe, T. Sekine, and M. Hase: *J. Phys. Soc. Jpn.* **81** (2012) 024711.
- [14] T. Hamasaki, H. Kuroe, T. Sekine, M. Hase, and H. Kitazawa: *J. Phys.: Conf. Ser.* **150** (2009) 042047.
- [15] S. Okubo, T. Yoshida, M. Fujisawa, T. Sakurai, H. Ohta, T. Hamasaki, H. Kuroe, T. Sekine, M. Hase, and K. Oka: *J. Low Temp. Phys.* **159** (2010) 32.
- [16] T. Hosaka, S. Hachiuma, H. Kuroe, T. Sekine, M. Hase, K. Oka, T. Ito, H. Eisaki, M. Fujisawa, S. Okubo, and H. Ohta: *J. Phys.: Conf. Ser.* **400** (2012) 032022.
- [17] W. J. Merz, *Phys. Rev.* **91** (1953) 513.
- [18] H. Kuroe, K. Aoki, R. Itoh, T. Hosaka, T. Hasegawa, M. Akaki, H. Kuwahara, T. Sekine M. Hase, K. Oka, T. Ito, and H. Eisaki: *J. Kor. Phys. Soc.* **63** (2013) 542.
- [19] K. Penc, N. Shannon, and H. Shiba: *Phys. Rev. Lett.* **93** (2004) 197203.
- [20] K. Penc, N. Shannon, and H. Shiba: *J. Phys.: Cond. Matter* **19** (2007) 145267.
- [21] E. Pytte: *Phys. Rev. B* **10** (1974) 4637.
- [22] M. Hase, I. Terasaki, and K. Uchinokura: *Phys. Rev. Lett.* **70** (1993) 3651.
- [23] Y. Kohama, Y. Hashimoto, S. Katsumoto, M. Tokunaga, and K. Kindo: *Meas. Sci. Technol.* **24** (2013) 115005.